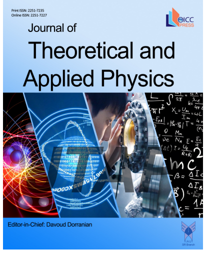

Volume 18, Issue 3, 182433 (1-7)

Journal of Theoretical and Applied Physics (JTAP)

https://dx.doi.org/10.57647/j.jtap.2024.1803.33

2D plasmonic micro-square arrays based on innovative two-step pattern transfer and plasma treatment for high-efficiency Si solar cells

Neda Roostaei[1], Seyedeh Mehri Hamidi[1,*], Guanghui-A. Chee[2,3,4]

[1] *Magneto-plasmonic Lab, Laser and Plasma Research Institute, Shahid Beheshti University, Tehran, Iran.*
[2] *National Education Center for Semiconductor Technology, Kyungpook National University, Daegu, Republic of Korea.*
[3] *Institute of Semiconductor Fusion Technology, Kyungpook National University, Daegu, Republic of Korea.*
[4] *School of Electronic and Electrical Engineering, Kyungpook National University, Daegu, Republic of Korea.*

[*]**Corresponding author:** m_hamidi@sbu.ac.ir

Original Research

Received:
19 April 2024
Revised:
13 May 2024
Accepted:
15 May 2024
Published online:
25 May 2024

Abstract:

Silicon (Si) photovoltaic cells and their production play a pivotal role in advancing energy utilization within the rapidly expanding solar industry, which serves as a critical driver in realizing global sustainability objectives and mitigating environmental repercussions associated with energy production. Here, we introduce a novel two-step pattern transfer technique to successfully imprint a two-dimensional plasmonic micro-square periodic array onto an Si substrate, utilizing Kapton® Tape and plasma technology. Remarkably, this represents the first-ever application of flexible and stretchable Kapton® polyimide for pattern transfer onto Si. The vacuum plasma treatment plays a pivotal role in significantly enhancing surface adhesion performance, thereby facilitating the efficient pattern transfer process. As a result, the resulting microstructure exhibits exceptional performance as a plamonic broadband absorber in the visible region, making it a highly promising candidate for enhancing efficiency in Si-based solar cells. To support our experimental findings, the finite-difference time domain method was employed for simulating the fabricated plasmonic structure and determining the electric field distribution. The simulation results unequivocally affirm the robust and intense light trapping capabilities of the microstructure. Moreover, our fabrication technique demonstrates the potential for achieving high-resolution microstructure through an innovative, straightforward, and cost-efficient approach.

Keywords: Plasmonic resonance; Surface lattice resonance; Optical absoption; Light trapping; Soft lithography

1. Introduction

The quest for more efficient solar cell technology has gained significant momentum in recent years, driven by the urgent need to harness renewable energy resources and mitigate climate change. Among the various strategies to enhance solar cell performance, light trapping has emerged as a critical aspect, aiming to maximize light absorption within the device and improve energy conversion efficiency. High-index materials, particularly semiconductor nanostructures, have garnered considerable attention as excellent candidates for achieving efficient light scattering, trapping, and localization. Silicon (Si), a widely used semiconductor in nanoelectronics and nanophotonics [1–3], holds a prominent position in the solar cell industry. The success of Si-based solar cells lies not only in its abundance but also in its well-established fabrication techniques developed in the nanoelectronics industry. These techniques have paved the way for large-scale, cost-effective production and seamless integration of photonic systems. Currently, crystalline Si-based solar cells dominate the solar energy market, accounting for 90% or more of photovoltaic devices in production. The solar cell industry places great emphasis on parameters, such as efficiency, cost, and stability. In this regard, Si-based solar cells utilizing crystalline Si as a high-quality light absorber offer an appealing choice owing to their non-toxicity, environmental friendliness, broad availability, exceptional stability, and extended operational lifetime. To push the limits of efficiency in Si-based solar cells, researchers have delved into various approaches, including the judicious application of charge carrier-selective contacts [4], defect engineering and control [5, 6], dopant and charge carrier optimization [5, 7], surface modifications [8], and the use of nanotechnology techniques [9, 10]. These endeavors have resulted in impressive achievements, with Si heterojunction solar cells reaching a maximum efficiency of 26.81% [11], approaching the theoretical maximum efficiency of 33% for single-junction photovoltaic systems [12]. This exceptional performance underscores the immense potential of Si-based solar cells in contributing to sustainable and clean energy solutions.

Thin films patterned with micro/nanostructures play a crucial role in determining the optical properties and light-trapping enhancement of solar cells [13, 14]. The effects of multiple scattering in periodic micro/nanostructures can significantly enhance optical absorption, with the scattered light effectively trapped within the substrate. The photophysical properties of the micro/nanostructures depend on their sizes, shapes/geometries, and periodicity. The ability of periodic Si-based micro/nanostructures to achieve tunable optical properties has attracted signficant interest across diverse applications, ranging from detector arrays [15], to solar cells [16–18], biosensing [19], and antireflection coatings [20]. One promising approach to further enhance optical absorption in photovoltaic cells is through light scattering by metal nanoparticles supporting localized surface plasmon resonance (LSPR) [21]. The plasmonic effect, arising from the collective oscillations of free electrons excited by incident light in the material, serves as a mechanism for enhancing photoabsorption in solar cells. This effect localizes optical waves within the nanostructure, leading to near-field and electromagnetic field enhancements. The extent of the plasmonic effect is contingent on the metal-dielectric interface morphology. In recent years, surface plasmon-enhanced solar cells have garnered significant attention from researchers due to their ease of construction, cost-effectiveness, and portability. Among these, plasmonic micro/nano-structures have received the most attention for their tunable resonance wavelength, high sensitivity, and affordability, leading to widespread adoption in both scientific research and industial applications. The efficient coupling of LSPR-enhanced local electromagnetic fields considerably boosts the device efficiency, while the subwavelength interactions of the micro/nano-structures supporting LSPR modes refine the broadband absoprtion characteristics.

Previous studies involving the incorporation of gold (Au) and silver nanoparticles into solar cells have demonstrated the vital role of plasmonic light trapping in boosting solar cell efficiency [22–24]. The periodic arrays of nanoparticles when their lattice structure is coupled with incident light leads to a resonance effect when the wavelength matches the periodicity of the nanostructure's lattice, thereby enhancing light-matter interactions and causing signficiant changes in the material's optical properties. Therefore, plasmonic micro/nanostructures provide a means to significantly increase light absorption and, thus, improve overall solar cell performance through the phenomenon of surface lattice resonances (SLRs). A variety of lithography techniques, including nanosphere, electron beam, focused ion beam, laser interference, nanoimprint, and anodic aluminium oxide template-based methods, have been employed for fabricating nanostructure arrays with specific minimum feature sizes and throughput characteristics [25]. Nevertheless, technical barreirs still exist to generate real nanostructures with long-range order periodic nanoarray patterns over large areas on substrates or solid-state chips at low-cost, and excellent controllability and repeatability. Furthermore, the integrated plasmonic metal-semiconductor heterojunctions required for plasmonic coupling between metals and semiconductors typically neccsitate high-temperature processing, which constrains the implementation of fabrication methods and pathways [25].

In this research, we present a novel and efficient two-step transfer technique that successfully imprints a two-dimensional (2D) micro-square periodic array onto an Si substrate. This innovative method, based on soft lithography, marks the first practical application of flexible and stretchable Kapton® Tape for pattern transfer onto Si. Kapton® Tape, renown for its excellent adhesion properties [26], plays a crucial role in facilitating the pattern transfer process. Furthermore, we employ vacuum plasma treatment to enhance surface bonding performance, further contributing to the seamless pattern transfer process. The resulting microstructure exhbits exceptional performance as a plasmonic broadband absorber in the visible region, thus presenting a highly promising solution for enhancing the efficiency in Si-based solar cells. In addition to experimental investigations, we performed detailed simulations of the fabricated plasmonic microstructure using finite-difference time-domain (FDTD) modeling to accurately calculate the electric field distribution. The simulation results unequivocally affirm the robust and intense light trapping capabilities of the microstructure, further validating the efficacy of our novel fabrication technique. Through the incorporating of high-index materials, particularly Si-based nanostructures, and the development of innovative fabrication techniques, this study signficantly contributes to the ongoing pursuit of high-efficiency light trapping materials and systems for next-generation solar cell technology. By harnessing the potential of these advancements, we can pave the way for more sustainable and effective solar energy utilization, driving us closer to cleaner and greener energy solutions.

2. Methods and materials

We successfully transferred a 2D periodic micro-square pattern onto an Si substrate employing an innovative, straightforward, and economically viable soft lithography technique. Figure 1(a) illustrates the pattern transfer process. This process involved utilizing a camera's charge-coupled device (CCD) as a stamp, possessing a 2D periodic micro-square pattern that has a periodicity of approximately 2.6 μm. To achieve this, careful extraction of the CCD from the camera was performed to preserve its surface integrity. Subsequently, consistent pressure was applied to firmly lam-

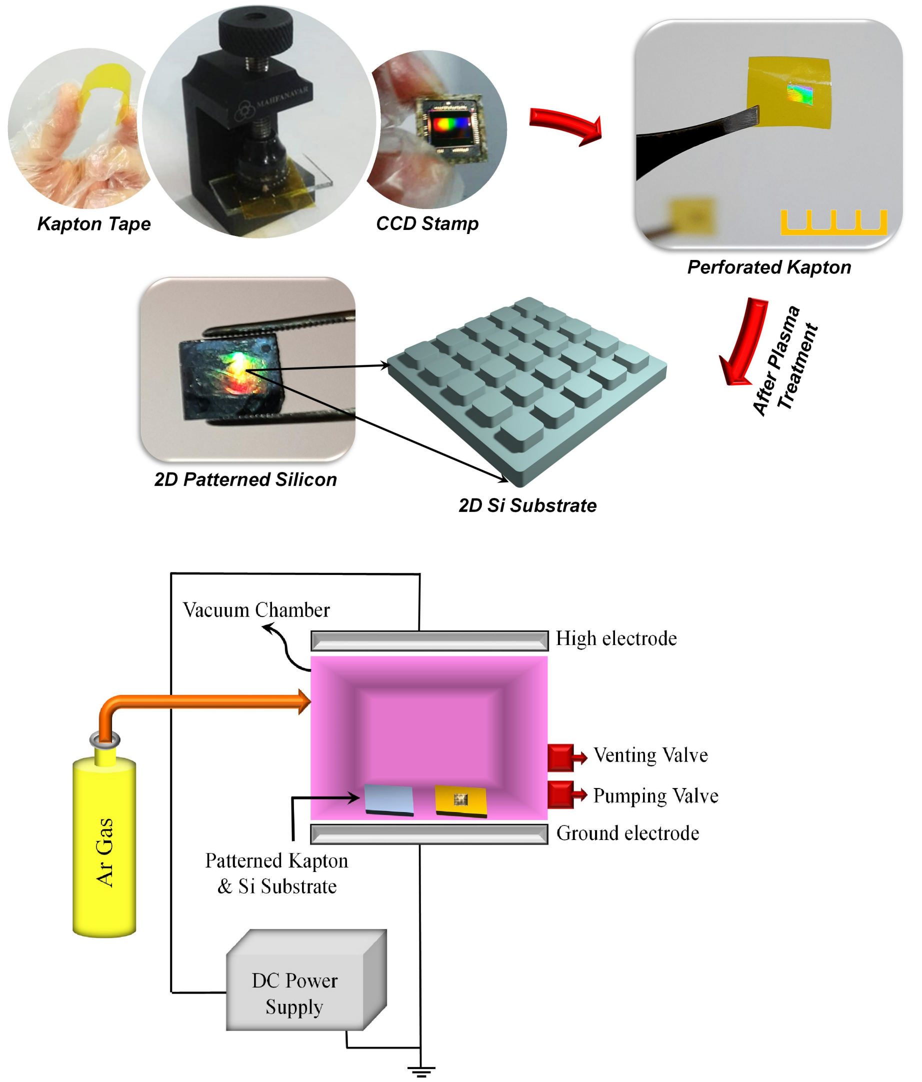

Figure 1. (a) Process flow diagram of the pattern transfer from the CCD stamp to the Si substrate, and the (b) experimental vacuum plasma treatment setup.

inate a film of Kapton® polyimide onto the optical CCD. The specimen was then subjected to a controlled heating process at 75 °C for 1 h to ensure the high-quality transfer of the pattern. To secure and stabilize the 2D micro-square array design onto the Kapton® Tape (see Figure 1(a)), a 24-h pressurization at ambient temperature was applied. In due course, the Kapton® Tape was gently stripped from the CCD stamp, resulting in the successful fabrication of a 2D flat and flexible microstructure based on Kapton® polyimide film (Figure 1(a)).

Next, the micro-imprinted Kapton® and Si substrate underwent a vacuum plasma treatment lasting a duration of 10 min. to effectively optimize the surface modification and improve adhesion properties. A schematic illustration of the surface activation process accomplished through plasma technology in the vacuum chamber is shown in Fig. 1(b). The experimental vacuum plasma setup consisted of a high voltage DC power supply, a vacuum chamber equipped with sample holder, hot and ground electrodes (dedicated to the Si substrate), gas feeding, and measurement systems. Grade 5 argon gas was introduced into the specimen chamber, elevating the pressure to 13.3 Pa, thereby initiating the plasma formation. Following plasma ignition, the pressure was subsequently reduced to approximately 0.53 Pa, thereby achieving the most favorable surface modification quality. The output of the DC power supply was adjusted to a voltage and current of 340 V and 40 mA, respectively, yielding a DC power of approximately 13.6 W. The potential difference between the electrodes accelerates the high-energy electrons and affects the gas molecules. These energetic collisions generate a cascade of free electrons and ions that can interact with the substrate surfaces, breaking the molecular bonds of the topmost layers. This procedure introduces active sites, polar groups, and reactive factor groups on the surface. During this process stage, surface modification occurs through a sequence of intricate reactions involving the participation of ions, atoms, molecules, free electrons, and radicals that form in the plasma. Consequently, the vaccuum plasma treatment significantly enhances the surface's hydrophilicity, activation, polarity, and adhesion qualities.

Following the plasma treatment, the patterned Kapton® polyimide Tape was methodically attached to the Si substrate, and the specimen was allowed to rest at room temperature for 1 h. Thereafter, the Kapton® Tape was carefully delaminated from the Si substrate, successfully transferring the 2D periodic micro-square array onto the Si surface (Figure 1(a)). Eventually, the two-dimensionally patterned Si substrate was coated with a 35 nm thin layer of Au using the DC sputter method. The physical vapor deposition was performed at a DC voltage of 365 V, plasma current of 0.01 mA, under a base pressure of 0.005 mbar, and substrate rotation speed of 28 rpm. This two-step process, involving Kapton® Tape and plasma technology, resulted in the successful fabrication of a 2D micro-square periodic array on the Si substrate. The surface morphology of the 2D micro-square periodic array was characterized using a variable-pressure scanning electron microscope (Hitachi SU3500). Reflectance-absorption spectroscopy was performed, both at a grazing angle and in the direct reflectance/absorption mode. The optical apparatus employed a robust micro-reflectivity setup to study the photophysical characteristics of the 2D plasmonic micro-structure surface. Unpolarized light emitted from an OSL2 fiber optic illuminator halogen lamp (Thorlabs, Newton, NJ, USA) consisting of wavelengths spanning from 400 to 700 nm was linearly polarized using a Glan-Taylor prism (GT10-A) to achieve transverse magnetic polarization. Subsequently, the polarized light-wave was precisely focused onto the specimen by means of an objective lens (Thorlabs), and the resulting reflected light was efficiently collected and coupled into an NANOCALC-XR UV-VIS spectrometer (Ocean Optics, Ostfildern, Germany) via an achromatic lens (Thorlabs). Ocean View 2.0 was the software utilized for rapid and stable data acquisition and processing.

To complement the experimental investigation, numerical simulations were conducted using Lumerical software and the FDTD method. Geometric specifications of the micro-structure were defined with one period per unit cell, featuring periodic boundary conditions in three dimensions. The refractive index values for Si and Au materials were extracted from the Palik [27] and Johnson and Christy [28] databases, respectively. For the achievement of desirable convergence characteristics, we utilized a 2 nm $\times$ 2 nm $\times$ 2 nm mesh size and applied a perfectly matched layer boundary condition to the edges of the micro-structure domain.

3. Results and discussion

Along with a schematic illustration of the sample cross-section, the fabricated sample consisting of the 2D micro-square periodic arrays patterned on a Si substrate is shown in Figure 2(a). The high-resolution secondary electron image in Figure 2 (b) showcases the morphology of the 2D plasmonic pattern on the Si substrate with a periodicity of 2.5 μm. The micro-square arrays exhibit high resolution 2D periodicity with excellent uniformity over the textured surface.

Figure 3(a) shows the absorption and normal reflection spectra from the 2D plasmonic Au/Si-based microstructure. Broadband absorption properties are demonstrated in the visible region, with an approximately 400-nm full width at half-maximum. This excellent plasmonic broadband absorber performance in the visible region indicates its potential application in Si-based solar cells to enhance efficiency. The normal reflection spectrum in Figure 3(a) also indicates weak reflection (and consequently strong absorption) within the visible range.

Periodically arranged metallic nanoparticles can give rise to distinctive narrow and strong excitations, pragmatically known as plasmonic SLR. This phenomenon arises from the coupling between the LSPRs generated by nanowires within each unit cell and the diffracted order (DO) waves in a stable structure. Figure 3(b) displays the reflection spectra measured at an optical incidence angle of 58° from both the 2D plasmonic Au/Si-based microstructure ($R_{2D\ Si/Au}$) and a planar Au-coated Si sample without any nanostructure patterning ($R_{Si/Au}$). Besides the redshift of spectral reflectance into the visible regime, the plasmonic resonance dip (see inset of Figure 3(b)), corresponding to the SLR phenomenon, was observed for the 2D plasmonic Au/Si microstructure. Notably, despite the sizable unit cell of the fabricated microstructure, characterized by a periodicity of the order of micrometers, thereby resulting in no direct matching between the incident light wavelength in the visible range and the lattice constant (periodicity), the experimental reflection spectra still revealed the presence of a distinctive SLR dip (Figure 3(b)). This intriguing phenomenon can be attributed to the effective coupling between the LSPR at the corners of each motif and the DO waves present in the 2D periodic

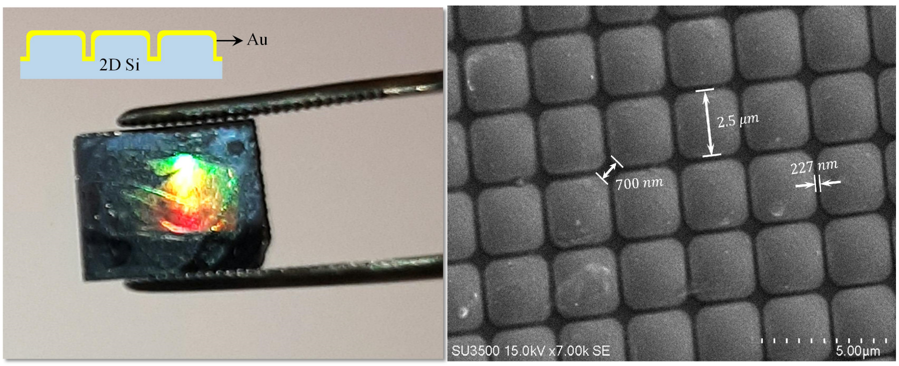

Figure 2. (a) Optical photograph of the fabricated Au/Si sample consisting of the 2D plasmonic microstructure on the Si substrate. The inset shows the cross-sectional depiction of the 2D plasmonic Au/Si nanostructure array. (b) High-resolution scanning electron microscopy micrograph of the fabricated sample.

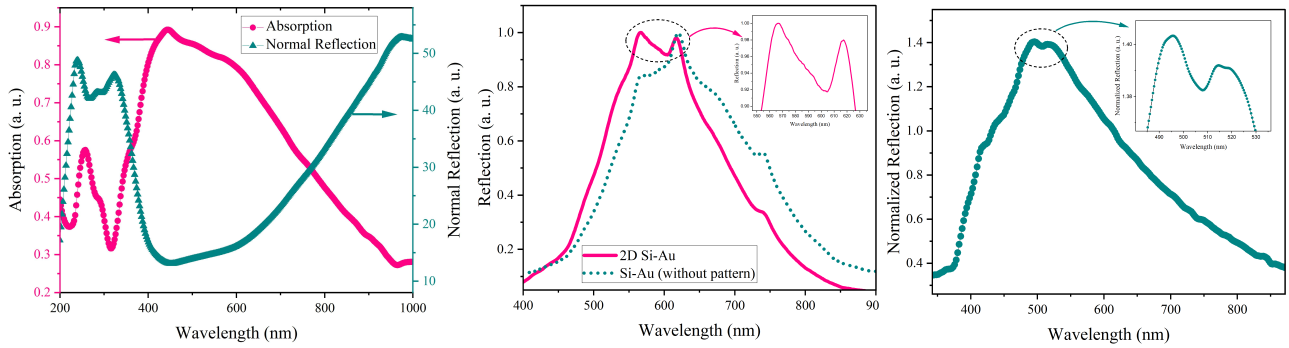

Figure 3. (a) Absorption and normal reflection spectra from the 2D plasmonic Au/Si microstructure. (b) Reflection spectra measured at an incidence angle of 58 from the 2D plasmonic Au/Si microstructure and Au-coated Si substrate without any patterning. (c) Normalized reflection spectra from the 2D plasmonic Au/Si microstructure, calculated by dividing the reflection data from the 2D plasmonic Au/Si microstructure by that from the simple Au-coated Si substrate without any patterning ($R_{2D\ Si/Au}/R_{Si/Au}$).

micro-square structure. Furthermore, the adjacent unit cells in the microstructure array are separated by approximately 227 nm (see Figure 2(b)). Each edge of the square lattice behaves like a wire, interacting with the commensurate wire of the unit cell neighbor, thus satisfying the plasmonic lattice resonance condition in the visible regime for the fabricated 2D periodic micro-square array. These findings underscore the significance of the plasmonic SLR in the microstructure, even in the presence of substantial unit cell dimensions and non-matching incident light wavelengths. The observed coupling mechanisms shed light on the intricate interactions that govern the optical behavior of such structures in the visible region. In contrast, the baseline planar Au/Si sample without any patterning did not exhibit any resonance (Figure 3(b)), as expected. In this case, the Si substrate was coated only with a thin film of Au, hence the surface lattice resonance condition was not satisfied.

To validate the SLR response, the normalized reflectance spectrum was derived by dividing $R_{2D\ Si/Au}$ by $R_{Si/Au}$, as shown in Figure 3(c). The resonant dip occurred at a wavelength of about 507.99 nm, confirming the plasmonic SLR effect. Notably, this resonance wavelength (507.99 nm) aligns with the absorption peak of the microstructure (see Figure 3(a)). Further in-depth analysis of the fabricated plasmonic Si-based microstructure involved simulation adopting the FDTD method to compute the electric field distribution. The simulated periodicity of the mistructure was determined based on experimental measurements from the SEM image (Figure 2(b)). Figure 4 illustrates the refractive index profile of a unit cell within the simulated 2D plasmonic microstructure and presents the corresponding electric field distribution at the resonance wavelength of 507.99 nm.

The electric field localization within the unit cell of the 2D plasmonic Au/Si-based micro-square array at the resonance wavelength of 507.99 nm confirms the strongly enhanced light trapping. This phenomenon results from the coupling between lattice surface modes (LSMs) in a perforated Si sub-

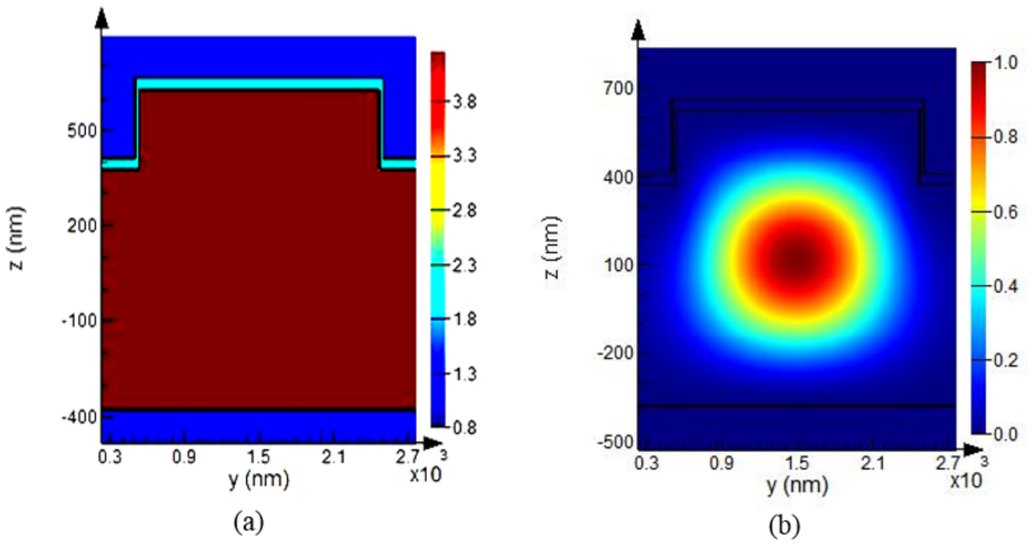

Figure 4. (a) Refractive index distribution and (b) the electric field profile within the simulated 2D plasmonic microstructure unit cell at the resonance wavelength of 507.99 nm.

strate and plasmonic SLR modes. The combination of LSM and SLR modes significantly enhances light trapping, making the Au/Si-based microstructure an excellent plasmonic broadband absorber in the visible region. Therefore, the plasmonic mechanism for the localized-field mediated photoresponse holds promise for application in high-efficiency Si-based solar cells. Furthermore, our innovative, simple design, and cost-efficient method of fabrication opens new possibilities for achieveing high-resolution microstructures, which can further enhance the performance of Si-based solar cells.

4. Conclusion

In this study, we presented an innovative two-step pattern transfer process, involving the successful transfer of a 2D micro-square periodic array onto a Si substrate using Kapton® Tape and vacuum plasma technology. Practically, this is the first demonstration of applying this method to pattern transfer from a CCD-stamped flexible and stretchable Kapton® polyimide film onto an Si substrate. We established that the vacuum plasma treatment plays a crucial role in surface modification, significantly enhancing the bonding performance and facilitating the pattern transfer process. Consequently, the fabricated 2D plasmonic micro-square array exhibits remarkable broadband absorption characteristics in the visible region, positioning it as a promising candidate for enhancing light trapping in Si-based solar cells.
Furthermore, we simulated the fabricated plasmonic structure using the FDTD method, enabling the investigation of the electric field distribution at the resonance wavelength. Both experimental and numerical results consistently confirm the presence of intense light trapping, attributed to the coupling between LSMs in a micro-patterned Si substrate and plasmonic SLR modes. These innovations represent a promising pathway in the development of surface plasmon excitation enhanced solar energy technology. With continued research and implementation of soft lithography plasmonic pattern transfer, we can unlock the full potential of high-efficiency, low-cost photovoltaic devices as a reliable source of power for a cleaner and more sustainable world.

Authors Contributions
All the authors have participated equally in the intellectual content, conception and design of this work or the analysis and interpretation of the data, as well as the writing of the manuscript.

Availability of data and materials
The datasets generated and analyzed during the current study are available from the corresponding author upon reasonable request.

Conflict of Interests
The author declare that they have no known competing financial interests or personal relationships that could have appeared to influence the work reported in this paper.

References

[1] A. H. Atabaki, S. Moazeni, F. Pavanello, H. Gevorgyan, J. Notaros, L. Alloatti, M. T. Wade, C. Sun, et al. "Integrating photonics with silicon nanoelectronics for the next generation of systems on a chip.". *Nature*, **556**:349–354, 2018. DOI: https://doi.org/10.1038/s41586-018-0028-z.

[2] S. Zaima. "Technology evolution for silicon nanoelectronics: Postscaling technology.". *Japanese Journal of Applied Physics*, **52**:030001, 2013. DOI: https://doi.org/10.7567/JJAP.52.030001.

[3] R. I. Bahar, D. Hammerstrom, J. Harlow, W. H. Joyner, C. Lau, D. Marculescu, A. Orailoglu, et al. "Architectures for silicon nanoelectronics and beyond.". *Computer*, **40**:25–33, 2007. DOI: https://doi.org/10.1109/MC.2007.7.

[4] T. G. Allen, J. Bullock, X. Yang, A. Javey, and S. De Wolf. "Passivating contacts for crystalline silicon solar cells.". *Nature Energy*, **4**:914–928, 2019. DOI: https://doi.org/10.1038/s41560-019-0463-6.

[5] M. Yamaguchi, T. Kamioka, N. Kojima, and Y. Ohshita. "Defect analysis of crystalline Si solar cells by learning radiation-induced defects in Si.". *MRS Communications*, **11**:272–277, 2021. DOI: https://doi.org/10.1557/s43579-021-00043-x.

[6] M. Wright, B. V. Stefani, A. Soeriyadi, R. Basnet, C. Sun, W. Weigand, Z. Yu, Z. Holman, et al. "Progress with defect engineering in silicon heterojunction solar cells.". *physica status solidi (RRL)–Rapid Research Letters*, **15**:2100170, 2021. DOI: https://doi.org/10.1002/pssr.202100170.

[7] G. C. Wilkes, A. D. Upadhyaya, A. Rohatgi, and M. C. Gupta. "Laser crystallization and dopant activation of a-Si:H Carrier-Selective layer in TOPCon Si solar cells.". *IEEE Journal of Photovoltaics*, **10**:1283–1289, 2020. DOI: https://doi.org/10.1109/JPHOTOV.2020.3006273.

[8] H. Park, M. Ju, M. Q. Khokhar, E. C. Cho, Y. Kim, Y. Cho, and J. Yi. "Surface modifications for light trapping in silicon heterojunction solar cells: A brief review. ". *Transactions on Electrical and Electronic Materials*, **21**:349–354, 2020. DOI: https://doi.org/10.1007/s42341-020-00203-1.

[9] L. C. Andreani, A. Bozzola, P. Kowalczewski, M. Liscidini, and L. Redorici. "Silicon solar cells: toward the efficiency limits. ". *Advances in Physics: X*, **4**:1548305, 2019. DOI: https://doi.org/10.1080/23746149.2018.1548305.

[10] K. W. A. Chee, Z. Tang, and F. Huang. "Anti-reflective structures for photovoltaics: Numerical and experimental design.". *Energy Reports*, **4**:266–273, 2018. DOI: https://doi.org/10.1016/j.egyr.2018.02.002.

[11] M. A. Green. " Silicon solar cells step up. ". *Nature Energy*, **8**:783–784, 2023. DOI: https://doi.org/10.1038/s41560-023-01296-7.

[12] I. M. Peters and T. Buonassisi. "Energy yield limits for single-junction solar cells. ". *Joule*, **2**:1160–1170, 2018. DOI: https://doi.org/10.1016/j.joule.2018.03.009.

[13] M. L. Brongersma, Y. Cui, and S. Fan. "Light management for photovoltaics using high-index nanostructures.". *Nature Materials*, **13**:451–460, 2014. DOI: https://doi.org/10.1038/nmat3921.

[14] H. A. Atwater and A. Polman. "Plasmonics for improved photovoltaic devices.". *Nature Materials*, **9**:205–213, 2010. DOI: https://doi.org/10.1038/nmat2629.

[15] A. H. Aldosari, M. Petasecca, A. Espinoza, M. Newall, I. Fuduli, C. Porumb, S. Alshaikh, Z. A. Alrowaili, M. Weaver, et al. "A two dimensional silicon detectors array for quality assurance in stereotactic radiotherapy: MagicPlate-512. ". *Medical Physics*, **41**:091707, 2014. DOI: https://doi.org/10.1118/1.4892384.

[16] C. Chen, R. Jia, H. Yue, H. Li, X. Liu, D. Wu, W. Ding, T. Ye, S. Kasai, H. Tamotsu, J. Chu, and S. Wang. "Silicon nanowire-array-textured solar cells for photovoltaic application.". *Journal of Applied Physics*, **108**:094318, 2010. DOI: https://doi.org/10.1063/1.3493733.

[17] S. A. Moiz, A. N. M. Alahmadi, and A. J. Aljohani. "Design of silicon nanowire array for PEDOT:PSS-Silicon nanowire-based hybrid solar cell.". *Energies*, **13**:3797, 2020. DOI: https://doi.org/10.3390/en13153797.

[18] P. Pei, S. T. Chang, C. W. Liu, and Y. C. Chen. "Numerical simulation on the photovoltaic behavior of an amorphous-silicon nanowire-array solar cell. ". *IEEE Electron Device Letters*, **30**:1305–1307, 2009. DOI: https://doi.org/10.1109/LED.2009.2033318.

[19] M. Lee and P. M. Fauchet. "Two-dimensional silicon photonic crystal based biosensing platform for protein detection. ". *Optics Express*, **15**:4530–4535, 2007. DOI: https://doi.org/10.1364/oe.15.004530.

[20] W. Ding, R. Jia, H. Li, Ch. Chen, Y. Sun, Z. Jin, and X. Liu. "Design of two dimensional silicon nanowire arrays for antireflection and light trapping in silicon solar cells.". *Journal of Applied Physics*, **115**:014307–5, 2014. DOI: https://doi.org/10.1063/1.4848996.

[21] N. Roostaei, H. Mbarak, S. A. Monfared, and S. M. Hamidi. "Plasmonic wideband and tunable absorber based on semi etalon nano structure in the visible region.". *Physica Scripta*, **96**:035805, 2021. DOI: https://doi.org/10.1088/1402-4896/abdbf6.

[22] D. Derkacs, S. H. Lim, P. Matheu, W. Mar, and E. T. Yu. "Improved performance of amorphous silicon solar cells via scattering from surface plasmon polaritons in nearby metallic nanoparticles. ". *Applied Physics Letters*, **89**:093103, 2006. DOI: https://doi.org/10.1063/1.2336629.

[23] D. M. Schaadt, B. Feng, and E. T. Yu. "Enhanced semiconductor optical absorption via surface plasmon excitation in metal nanoparticles.". *Applied Physics Letters*, **86**:063106, 2005. DOI: https://doi.org/10.1063/1.1855423.

[24] S. Pillai, K. Catchpole, T. Trupke, and M. Green. "Surface plasmon enhanced silicon solar cells. ". *Journal of Applied Physics*, **101**:093105–8, 2007. DOI: https://doi.org/10.1063/1.2734885.

[25] S. Kasani, K. Curtin, and N. Wu. "A review of 2D and 3D plasmonic nanostructure array patterns: fabrication, light management and sensing applications.". *Nanophotonics*, **8**:2065–2089, 2019. DOI: https://doi.org/10.1515/nanoph-2019-0158.

[26] N. Roostaei and S. M. Hamidi. "Flat and flexible 2D plasmonic crystal for color production.". *International Journal of Optics and Photonics*, **15**:93–100, 2021. DOI: https://doi.org/10.52547/ijop.15.1.93.

[27] D. F. Edwards. "Silicon (Si)**Work performed under the auspices of the U.S. Department of Energy, in Handbook of Optical Constants of Solids,.". *Academic Press: Boston*, :547–569, 1985.

[28] P. B. Johnson and R. W. Christy. "Optical Constants of the Noble Metals. ". *Physical Review B*, **6**:4370–4379, 1972. DOI: https://doi.org/10.1103/PhysRevB.6.4370.